

Pion photoproduction on nucleus with two-nucleon emission

Glavanakov I.V., Tabachenko A.N.

*Institute of Physics and Technology, Tomsk Polytechnic University,
634050, Tomsk, Russia*

A model for the pion photoproduction on nuclei in the $A(\gamma, \pi NN)B$ reaction is presented. This is an extension of our recent model for the $A(\gamma, \pi N)B$ reaction. In this approach we have moved beyond the standard shell-model considering ΔN correlations in the nuclear wave functions, which are caused by the virtual transitions $NN \rightarrow \Delta N \rightarrow NN$ in the ground state of the nucleus. The main ingredients of the model are the two- and three-particle density matrices and the transition operators $\gamma\Delta \rightarrow N\pi$ and $\gamma N \rightarrow N\pi$. The direct and exchange reaction mechanisms, which follow from the structure of the density matrices, are examined. The model is used to investigate the $^{12}\text{C}(\gamma, \pi^+p)$ and $^{12}\text{C}(\gamma, \pi^-p)$ reactions in the kinematic region of the large momentum transfers to the residual nuclear system, where the pion production occurs with the emission of two nucleons.

1 Introduction

In nuclear physics, one of the important problems is the study of the nuclear structure at short and medium inter-nucleon distances, where the effects of the non-nucleon degrees of freedom in nuclei appear. The short- and middle-range structure of nuclei is defined by the short- and middle-range components of the nucleon-nucleon potential, which lead to the high-momentum components of the nuclear wave function. These wave function components have a low probability. However, there are nuclear processes which in the selected kinematic regions are almost completely caused by these components of the wave function, which allows the various manifestations of the non-nucleon degrees of freedom in nuclei to be studied.

As is known, the two-nucleon knockout electromagnetic processes are a powerful tool for studying the short- and middle- range dynamics of the interaction between nucleons in nuclei.

In the framework of the independent particle model, the knocking-out from the nucleus of two nucleons can occur by means of the two-body operators corresponding to the meson exchange and isobar currents.

Another two-nucleon knockout mechanism is based on the nucleus model, in which the correlated pairs of nucleons in the nucleus are taken into account. This model is beyond the framework of the independent particle model. The correlation of nucleons in the nucleus is described by the correlation function, which reflects the structure of the nucleon-nucleon potential. The process of knocking out nucleons in this model is due to the action of the single-particle operator. As a result of knocking out either nucleon, the second nucleon of the correlated pair can move to a free state.

Today these two approaches are widely used in the analysis of the knockout ($e, e'NN$) reactions, which is oriented mainly to the study of short-range correlations induced by the repulsive part of the nucleon-nucleon potential at small distances [1].

Another type of two-particle correlation in the nucleus is associated with the virtual transitions $NN \rightarrow \Delta N \rightarrow NN$ in the ground state of the nucleus. The interaction of the incident particle with the correlated ΔN system may also lead to the knockout of two nucleons. These ΔN correlations correspond to the middle-range components of the nucleon-nucleon potential.

The role and relevance of these three competing processes can be different in different reactions and kinematics. The peculiarity of manifestations of the ΔN -correlations in nuclear reactions consists in the fact that the knocking-out of the Δ -isobar causes production of a pion as a result of $\Delta \rightarrow N\pi$ decay. Therefore, because of the particle type in the final state, the $(\gamma, \pi NN)$ reactions are more sensitive to the manifestations of the correlation of this type.

This article presents the analysis of the $A(\gamma, \pi NN)B$ process, taking into account the ΔN -correlations in the ground state of the nucleus. The method of analysis is an extension of the approach, developed in [2, 3] for the process $(\gamma, \pi N)$ at large momentum transfer, to pion photoproduction with the two-nucleon knockout. The direct and exchange reaction mechanisms are considered.

2 Cross-section of the $A(\gamma, \pi NN)B$ reaction

The differential cross-section reaction

$$A(\gamma, \pi NN)B$$

can be written in the laboratory system of coordinates as

$$d\sigma = 2\pi\delta(E_\gamma + M_T - E_\pi - E_1 - E_2 - E_R) \times \frac{|T_{fi}|^2}{4E_\gamma E_\pi} \frac{d\mathbf{p}_\pi}{(2\pi)^3} \frac{d\mathbf{p}_1}{(2\pi)^3} \frac{d\mathbf{p}_2}{(2\pi)^3} \frac{d\mathbf{p}_R}{(2\pi)^3},$$

where $(E_\gamma, \mathbf{p}_\gamma)$, (E_π, \mathbf{p}_π) , (E_1, \mathbf{p}_1) , (E_2, \mathbf{p}_2) , and (E_R, \mathbf{p}_R) are the four-momenta of the photon, pion, two nucleons, and the residual nucleus B ; M_T is the mass of the nucleus A ; T_{fi} is the transition matrix element from the initial state, which includes the photon and the nucleus A , to the final, including the pion, two nucleons in a free state and the residual nucleus B .

The matrix element can be represented in the form

$$T_{fi} = A \int d(X'_1, X_1, X_2, \dots, X_A) \Psi_F^*(X'_1, X_2, \dots, X_A) \times \langle X'_1 | t_{\gamma\pi} | X_1 \rangle \Psi_T(X_1, X_2, \dots, X_A).$$

Here Ψ_T and Ψ_F are the wave functions of the nucleus A and the system F , which includes the free nucleons and the residual nucleus B ; $t_{\gamma\pi}$ is the single-particle operator of the pion photoproduction on free baryons; X_i is the coordinate in some space X , fully characterizing

the position of the i -th particle; and the integral means the summation over the discrete and integration over the continuous variables.

Writing the wave function Ψ_F as the antisymmetrized product of the wave function $\phi_{\alpha_1\alpha_2}$, describing the state of two free nucleons ($\alpha \equiv \mathbf{p}, m\sigma, m\tau$ is the nucleon state index), and the wave function of the residual nucleus, we obtain the following expression for T_{fi}

$$T_{fi} = T_d - T_e,$$

where

$$T_d = (2A(A-1))^{1/2} \int d(X'_1, X_1, X_2, \dots, X_A) \phi_{\alpha_1\alpha_2}^*(X'_1, X_2) \\ \times \Psi_f^*(X_3, X_4, \dots, X_A) \langle X'_1 | t_{\gamma\pi} | X_1 \rangle \Psi_T(X_1, X_2, \dots, X_A)$$

is the direct amplitude, in which the particle with the coordinate X'_1 is a free nucleon, and

$$T_e = \left(\frac{A(A-1)}{2} \right)^{1/2} (A-2) \int d(X'_1, X_1, X_2, \dots, X_A) \phi_{\alpha_1\alpha_2}^*(X_3, X_2) \\ \times \Psi_f^*(X'_1, X_4, \dots, X_A) \langle X'_1 | t_{\gamma\pi} | X_1 \rangle \Psi_T(X_1, X_2, \dots, X_A) \quad (1)$$

is the exchange amplitude, in which the particle with the coordinate X'_1 is the part of the residual nucleus.

Consider the square of the modulus of the matrix element T_{fi}

$$|T_{fi}|^2 = |T_d|^2 + |T_e|^2 - 2Re(T_d T_e^*). \quad (2)$$

We are interested in differential cross-sections of the $A(\gamma, \pi NN)B$ reaction, summed over the states of the residual nucleus. Assuming that the set of states of the residual nucleus possesses the completeness, the square of the modulus of the direct amplitude T_d can be expressed as

$$\sum_f |T_d|^2 = 2A(A-1) \int d(X'_1, X_1, X_2, \tilde{X}'_1, \tilde{X}_1, \tilde{X}_2) \phi_{\alpha_1\alpha_2}^*(X'_1, X_2) \\ \times \langle X'_1 | t_{\gamma\pi} | X_1 \rangle \rho(X_1, X_2; \tilde{X}_1, \tilde{X}_2) \\ \times \langle \tilde{X}_1 | t_{\gamma\pi}^+ | \tilde{X}'_1 \rangle \phi_{\alpha_1\alpha_2}(\tilde{X}'_1, \tilde{X}_2), \quad (3)$$

where

$$\rho(X_1, X_2; \tilde{X}_1, \tilde{X}_2) = \int d(X_3, X_4, \dots, X_A) \\ \times \Psi_T(X_1, X_2, X_3, \dots, X_A) \Psi_T^*(\tilde{X}_1, \tilde{X}_2, X_3, \dots, X_A) \quad (4)$$

is the two-particle density matrix.

Under the production of a charged pion by means of the exchange reaction mechanism the "active" nucleon will most likely move to the level above the Fermi level. In this case, the wave function of the residual nucleus can be written as

$$\Psi_f(X'_1, X_4, \dots, X_A) = A_{u;1\dots A \neq klm}^s \Psi_{\beta_u}(X'_1) \Psi_{(\beta_k\beta_l\beta_m)^{-1}}(X_4, \dots, X_A),$$

where the antisymmetrization operator $A_{u;1\dots A}^s$ rearranges the indices of the particle states, β_u is the index of the state of the nucleon above the Fermi level, and $(\beta_k\beta_l\beta_m)^{-1}$ is the hole state of the bound system of particles with the numbers 4, ..., A . As a result, assuming that the set of the hole states is complete, we obtain

$$\begin{aligned} \sum_f |T_e|^2 &= \frac{A(A-1)(A-2)}{2} \sum_u \int d(X'_1, X_1, X_2, X_3, \tilde{X}'_1, \tilde{X}_1, \tilde{X}_2, \tilde{X}_3) \\ &\times \phi_{\alpha_1\alpha_2}^*(X_3, X_2) \Psi_{\beta_u}^*(X'_1) \langle X'_1 | t_{\gamma\pi} | X_1 \rangle \rho(X_1, X_2, X_3; \tilde{X}_1, \tilde{X}_2, \tilde{X}_3) \\ &\times \langle \tilde{X}_1 | t_{\gamma\pi}^+ | X'_1 \rangle \Psi_{\beta_u}(\tilde{X}'_1) \phi_{\alpha_1\alpha_2}(\tilde{X}_3, \tilde{X}_2). \end{aligned} \quad (5)$$

Here

$$\begin{aligned} \rho(X_1, X_2, X_3; \tilde{X}_1, \tilde{X}_2, \tilde{X}_3) &= \int d(X_4, \dots, X_A) \\ &\times \Psi_T(X_1, X_2, X_3, \dots, X_A) \Psi_T^*(\tilde{X}_1, \tilde{X}_2, \tilde{X}_3, X_4, \dots, X_A) \end{aligned}$$

is the three-body density matrix.

Since the kinematic region where the main contributions of the direct and exchange amplitudes are significantly different, in calculating the square of the modulus T_{fi} , we neglect in (2) the product $T_d T_e^*$.

3 The basic assumptions of the model

We analyse the reaction $A(\gamma, \pi NN)B$ in the framework of the formalism developed in [4] for the description of the ground state of nuclei, which previously we used in [2, 3] for considering the reaction $A(\gamma, \pi N)B$ – pion photoproduction with the emission of a single nucleon. According to [4], baryons bound in the nucleus, in addition to the space \mathbf{r} , spin s , and isospin t coordinates ($r, s, t \equiv x$), are also characterized by the intrinsic coordinate m ($x, m \equiv X$). An eigenfunction $\Psi_\beta(X_1, \dots, X_A)$ of the Hamiltonian H of the system A particles with eigenvalue E_β is a superposition of the wave functions concerned with different intrinsic configurations

$$\Psi_\beta(X_1, \dots, X_A) = \sum_n A_n \varphi_n(m_1, \dots, m_A) \Psi_\beta^n(x_1, \dots, x_A).$$

Here $\Psi_\beta^n(x_1, \dots, x_A)$ is the wave function describing the state of A particles in the usual, spin, and isospin spaces; $\varphi_n(m_1, \dots, m_A)$ is the wave function describing the intrinsic states of baryons. The index $\beta \equiv \beta_1, \dots, \beta_A$ characterizes the usual space and the spin and isospin states of A particles. The index $n \equiv n_1, \dots, n_A$ defines the intrinsic states of the particles. For instance, the state index describing the intrinsic configuration of the nucleon system is written as $n = N_1, N_2, \dots, N_A$; if the first particle is in the isobar state, but the rest are nucleons, the intrinsic state index is written as $n = \Delta_1, N_2, \dots, N_A$. The wave function $\Psi_\beta^n(x_1, \dots, x_A)$ should be antisymmetric for particles in the same intrinsic state. The remaining antisymmetrization for particles in different intrinsic states is done by the operator A_n . The wave functions $\varphi_n(m_1, \dots, m_A)$ satisfy the condition

$$\sum_{m_1, \dots, m_A} \varphi_n(m_1, \dots, m_A) \varphi_n^*(m_1, \dots, m_A) = \delta_{n_1, \tilde{n}_1} \cdot \dots \cdot \delta_{n_A, \tilde{n}_A}.$$

In our model, we will consider the two intrinsic configurations: a configuration in which all the particles are nucleons and an isobar configuration, in which one particle is Δ -isobar and the others are nucleons,

$$\Psi_T = \Psi_T^N + \Psi_T^\Delta.$$

Here Ψ_T^N and Ψ_T^Δ are the wave functions of the nucleon and isobar configurations.

Assuming that only two nucleons are involved in the excitation of the nucleon's internal degrees of freedom, the wave function $\Psi_T^\Delta(X_1, \dots, X_A)$ of the isobar configuration can be written as the superposition of the products of the wave function $\Psi_{[\beta_i\beta_j]}^{\Delta N}(X_1, X_2)$ of the ΔN system, which includes an isobar and the second nucleon (the participant of the transition $NN \rightarrow \Delta N$) and the wave function $\Psi_{(\beta_i\beta_j)^{-1}}^N(X_3, \dots, X_A)$, describing the state of the nucleon core, which includes other $A-2$ nucleons,

$$\Psi_T^\Delta(X_1, \dots, X_A) = A_{12;3\dots A} \sum_{ij} \Psi_{[\beta_i\beta_j]}^{\Delta N}(X_1, X_2) \Psi_{(\beta_i\beta_j)^{-1}}^N(X_3, \dots, X_A). \quad (6)$$

Here

$$A_{12;3\dots A} = \left(\frac{2}{A(A-1)} \right)^{1/2} \left[1 - \sum_{i=3}^A (P_{1i} + P_{2i}) + \sum_{i=3}^{A-1} \sum_{j=i+1}^A P_{1i} P_{2j} \right]$$

is the antisymmetrization operator; the operator P_{ik} interchanges the i -th and k -th nucleons,

$$\Psi_{[\beta_i\beta_j]}^{\Delta N}(X_1, X_2) = A_{1;2} \varphi_{\Delta N}(m_1, m_2) \Psi_{[\beta_i\beta_j]}^{\Delta N}(x_1, x_2),$$

$$\Psi_{(\beta_i\beta_j)^{-1}}^N(X_3, \dots, X_A) = \varphi_{N\dots N}(m_3, \dots, m_A) \Psi_{(\beta_i\beta_j)^{-1}}^N(x_3, \dots, x_A).$$

The oscillator shell model is used to describe the state of the $A-2$ nucleons. The wave function of the ΔN -system is the solution of the Schrödinger equation for the potential due to the exchange of π - and ρ -mesons, which describes the transition process $NN \rightarrow \Delta N$ [4, 5].

According to (3) and (5) the square of the modulus of both the direct and exchange amplitudes are expressed in terms of the density matrix and the matrix elements of the single-particle operator of pion production $t_{\gamma\pi}$.

Considering the elementary processes, we take into account the reaction mechanisms, which correspond to the single-particle transitions $\gamma N \rightarrow N\pi$ and $\gamma\Delta \rightarrow N\pi$. We shall use the non-relativistic operator of Blomqvist-Laget [6] as the single-particle transition operator $\gamma N \rightarrow N\pi$, which acts on the usual space, spin, and isospin variables and is defined as

$$\langle x' | t_{\gamma N\pi} | x \rangle = \sum_{m', m} \varphi_N^*(m') \langle X' | t_{\gamma\pi} | X \rangle \varphi_N(m).$$

Using the S -matrix approach to the description of the $\gamma + \Delta \rightarrow N + \pi$ processes, the transition operator $\gamma\Delta \rightarrow N\pi$

$$\langle x' | t_{\gamma\Delta\pi} | x \rangle = \sum_{m', m} \varphi_N^*(m') \langle X' | t_{\gamma\pi} | X \rangle \varphi_\Delta(m)$$

was found. Let us to write it as an expansion on the four spin and three isospin independent structures with the expansion coefficients, which depend on the coupling constants and magnetic moments [2]. The explicit form can be written as

$$\langle x' | t_{\gamma\Delta\pi} | x \rangle = \delta(r' - r) e^{i(p_\gamma r - p_\pi r')} \langle s', t' | t_{\gamma\Delta\pi} | s, t \rangle.$$

Here

$$t_{\gamma\Delta\pi} = \phi_a^+ \sum_{i=1}^4 \sum_{j=1}^3 f_{ij} M_i I_j,$$

where ϕ_a is the covariant unit vector of the cyclical basis describing the isotopic state of the pion; index a takes on the values $+$, 0 , and $-$, which fit with the positive, neutral, and negative pions; M_i are the independent spin structures

$$\begin{aligned} M_1 &= \boldsymbol{\varepsilon}^\lambda \cdot \mathbf{S}^+; & M_2 &= i\boldsymbol{\sigma} \cdot [\mathbf{p}_\gamma \times \boldsymbol{\varepsilon}^\lambda] \mathbf{p}_\pi \cdot \mathbf{S}^+; \\ M_3 &= \mathbf{p}_\pi \cdot \boldsymbol{\varepsilon}^\lambda \mathbf{p}_\gamma \cdot \mathbf{S}^+; & M_4 &= \mathbf{p}_\pi \cdot \boldsymbol{\varepsilon}^\lambda \mathbf{p}_\pi \cdot \mathbf{S}^+. \end{aligned}$$

Here $\boldsymbol{\varepsilon}^\lambda$ is the three-vector of the photon polarization; $\boldsymbol{\sigma}$ is the Pauli matrix; \mathbf{S}^+ is the transition spin operator, which converts the spin-3/2 state into the spin-1/2 state.

The isospin structures are

$$\mathbf{I}_1 = \mathbf{T}^+, \quad \mathbf{I}_2 = \boldsymbol{\tau}T_3^+, \quad \mathbf{I}_3 = \tau_3\mathbf{T}^+$$

, where $\boldsymbol{\tau}$ and \mathbf{T}^+ are analogues $\boldsymbol{\sigma}$ and \mathbf{S}^+ in isotopic space. Value f_{ij} is a function of the photon and pion momenta, the coupling constants πNN , $\pi N\Delta$, $\pi\Delta\Delta$, the magnetic moments of the nucleon and Δ -isobar, and the transition magnetic moment $\mu_{\gamma N\Delta}$. The explicit form of f_{ij} and the used values of the coupling constants and the magnetic moments are given in [2].

4 Density matrices

In this approach, according to (3) and (5), all information about the structure of the nucleus and the mechanism of the $A(\gamma, \pi NN)B$ reaction is contained in the two- and three-body density matrices.

The two-particle density matrix $\rho(X_1, X_2; \tilde{X}_1, \tilde{X}_2)$ (4) contained in the expression for the square of the modulus of the direct amplitude (3) of the $A(\gamma, \pi NN)B$ reaction was also used to describe the exchange mechanisms of the pion production in the reaction $A(\gamma, \pi N)B$ [2]. We are interested in the isobar configurations in the ground state of the nucleus, so we consider the density matrix

$$\begin{aligned} \rho^\Delta(X_1, X_2; \tilde{X}_1, \tilde{X}_2) &= \int d(X_3, X_4, \dots, X_A) \\ &\times \Psi_T^\Delta(X_1, X_2, X_3, \dots, X_A) \Psi_T^{\Delta*}(\tilde{X}_1, \tilde{X}_2, X_3, \dots, X_A). \end{aligned}$$

Substituting in this expression the wave functions of the isobar configuration presented in the form (6), and integrating over X_3, \dots, X_A , we obtain, according to [2]

$$\rho^\Delta(X_1, X_2; \tilde{X}_1, \tilde{X}_2) = \rho_{\Delta N} + \rho_{N\Delta} + \rho_{\Delta C} + \rho_{NC} + \rho_{CN} + \rho_{C\Delta} + \rho_{CC}.$$

Here, the two lower indices of the density matrix determine the state of the particles with the numbers 1 and 2. Indices Δ , N , or C respectively indicate that the particle is a Δ -isobar or a nucleon of the ΔN system, or belongs to the nucleon core.

Because of the orthogonality of the wave functions φ_N and φ_Δ , the direct amplitudes corresponding to the matrices $\rho_{N\Delta}$ and $\rho_{C\Delta}$ according to (3) are zero. In the amplitude corresponding to the ρ_{CC} matrix, the ΔN system is a part of the residual nucleus and does not dynamically manifest itself. This amplitude contributes to the cross-section in a range of the low momentum transfer, where the quasi-free pion photoproduction is dominant, so it will not be considered. The remaining four terms $\rho_{\Delta N}$, $\rho_{\Delta C}$, ρ_{NC} , and ρ_{CN} of the two-particle density matrix

$$\begin{aligned}
\rho_{\Delta N} & \left(X_1, X_2; \tilde{X}_1, \tilde{X}_2 \right) = \varphi_{\Delta N} (m_1, m_2) \\
& \times \left[\frac{1}{A(A-1)} \sum_{ij} \Psi_{[\beta_i\beta_j]}^{\Delta N} (x_1, x_2) \Psi_{[\beta_i\beta_j]}^{\Delta N*} (\tilde{x}_1, \tilde{x}_2) \right] \varphi_{\Delta N}^* (\tilde{m}_1, \tilde{m}_2), \\
\rho_{\Delta C} & \left(X_1, X_2; \tilde{X}_1, \tilde{X}_2 \right) \\
& = \varphi_{\Delta N} (m_1, m_2) \left[\frac{1}{A(A-1)} \sum_{ij, k \neq ij} \int d(x_3) \Psi_{[\beta_i\beta_j]}^{\Delta N} (x_1, x_3) \Psi_{\beta_k} (x_2) \right. \\
& \quad \left. \times \Psi_{\beta_k}^* (\tilde{x}_2) \Psi_{[\beta_i\beta_j]}^{\Delta N*} (\tilde{x}_1, x_3) \right] \varphi_{\Delta N}^* (\tilde{m}_1, \tilde{m}_2), \\
\rho_{NC} & \left(X_1, X_2; \tilde{X}_1, \tilde{X}_2 \right) \\
& = \varphi_{NN} (m_1, m_2) \left[\frac{1}{A(A-1)} \sum_{ij, k \neq ij} \int d(x_3) \Psi_{[\beta_i\beta_j]}^{\Delta N} (x_3, x_1) \Psi_{\beta_k} (x_2) \right. \\
& \quad \left. \times \Psi_{\beta_k}^* (\tilde{x}_2) \Psi_{[\beta_i\beta_j]}^{\Delta N*} (x_3, \tilde{x}_1) \right] \varphi_{NN}^* (\tilde{m}_1, \tilde{m}_2), \\
\rho_{CN} & \left(X_1, X_2; \tilde{X}_1, \tilde{X}_2 \right) \\
& = \varphi_{NN} (m_1, m_2) \left[\frac{1}{A(A-1)} \sum_{ij, k \neq ij} \int d(x_3) \Psi_{[\beta_i\beta_j]}^{\Delta N} (x_3, x_2) \Psi_{\beta_k} (x_1) \right. \\
& \quad \left. \times \Psi_{\beta_k}^* (\tilde{x}_1) \Psi_{[\beta_i\beta_j]}^{\Delta N*} (x_3, \tilde{x}_2) \right] \varphi_{NN}^* (\tilde{m}_1, \tilde{m}_2)
\end{aligned}$$

correspond to the reaction mechanisms, which are illustrated by the diagrams shown in Fig. 1.

The correspondence between the individual terms of the density matrix and diagrams in Fig. 1 is a simple one: the photon interacts with a baryon 1, which together with a baryon 2 goes to a free state; baryons, over whose coordinates the integration is carried out, are part of the residual nucleus. Each term of the density matrix corresponds to the appointed final state, which depends on the structure of the matrix and the $\langle X'_1 | t_{\gamma\pi} | X_1 \rangle$ operator.

We now consider the three-particle density matrix

$$\begin{aligned}
\rho^\Delta & \left(X_1, X_2, X_3; \tilde{X}_1, \tilde{X}_2, \tilde{X}_3 \right) = \int d(X_4, \dots, X_A) \\
& \times \Psi_T^\Delta (X_1, X_2, X_3, X_4, \dots, X_A) \Psi_T^{\Delta*} (\tilde{X}_1, \tilde{X}_2, \tilde{X}_3, X_4, \dots, X_A).
\end{aligned}$$

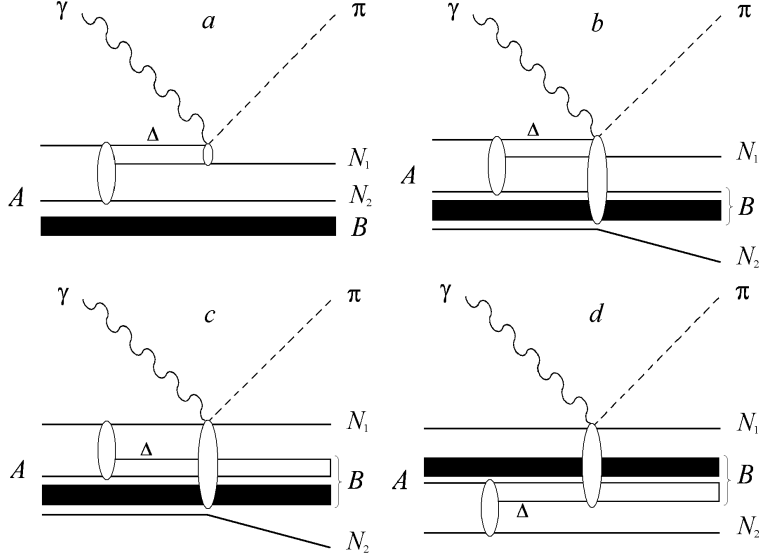


Figure 1: Diagrams illustrating the direct mechanisms of the pion photoproduction on nuclei in the $A(\gamma, \pi NN)B$ reaction.

The expression for ρ^Δ can be represented as a sum of five terms, as a result of the transformation, similar to that carried out with the two-particle density matrix

$$\rho^\Delta = \rho_{CSS} + \rho_{SSC} + \rho_{SCC} + \rho_{CSC} + \rho_{CCC},$$

where

$$\begin{aligned} \rho_{CSS} \left(X_1, X_2, X_3; \tilde{X}_1, \tilde{X}_2, \tilde{X}_3 \right) &= \frac{2}{A(A-1)(A-2)} \\ &\times \sum_{ij, k \neq ij} \Psi_{\beta_k} (X_1) \Psi_{[\beta_i \beta_j]}^{\Delta N} (X_2, X_3) \Psi_{[\beta_i \beta_j]}^{\Delta N^*} \left(\tilde{X}_2, \tilde{X}_3 \right) \Psi_{\beta_k}^* \left(\tilde{X}_1 \right), \\ \rho_{SSC} \left(X_1, X_2, X_3; \tilde{X}_1, \tilde{X}_2, \tilde{X}_3 \right) &= \frac{4}{A(A-1)(A-2)} \\ &\times \sum_{ij, k \neq ij} \Psi_{\beta_k} (X_3) \Psi_{[\beta_i \beta_j]}^{\Delta N} (X_1, X_2) \Psi_{[\beta_i \beta_j]}^{\Delta N^*} \left(\tilde{X}_1, \tilde{X}_2 \right) \Psi_{\beta_k}^* \left(\tilde{X}_3 \right), \\ \rho_{SCC} \left(X_1, X_2, X_3; \tilde{X}_1, \tilde{X}_2, \tilde{X}_3 \right) &= \frac{4}{A(A-1)(A-2)} \sum_{ij, kl \neq ij} \Psi_{\beta_k \beta_l} (X_2, X_3) \\ &\times \int d(X_4) \Psi_{[\beta_i \beta_j]}^{\Delta N} (X_1, X_4) \Psi_{[\beta_i \beta_j]}^{\Delta N^*} \left(\tilde{X}_1, X_4 \right) \Psi_{\beta_k \beta_l}^* \left(\tilde{X}_2, \tilde{X}_3 \right), \\ \rho_{CSC} \left(X_1, X_2, X_3; \tilde{X}_1, \tilde{X}_2, \tilde{X}_3 \right) &= \frac{8}{A(A-1)(A-2)} \sum_{ij, kl \neq ij} \Psi_{\beta_k \beta_l} (X_1, X_3) \\ &\times \int d(X_4) \Psi_{[\beta_i \beta_j]}^{\Delta N} (X_2, X_4) \Psi_{[\beta_i \beta_j]}^{\Delta N^*} \left(\tilde{X}_2, X_4 \right) \Psi_{\beta_k \beta_l}^* \left(\tilde{X}_1, \tilde{X}_3 \right), \\ \rho_{CCC} \left(X_1, X_2, X_3; \tilde{X}_1, \tilde{X}_2, \tilde{X}_3 \right) &= \frac{6}{A(A-1)(A-2)} \end{aligned}$$

$$\times \sum_{ij,klm \neq ij} \Psi_{\beta_k \beta_l \beta_m}^{\Delta N} (X_1, X_2, X_3) \int d(X_4, X_5) \Psi_{[\beta_i \beta_j]}^{\Delta N} \Psi_{[\beta_i \beta_j]}^{\Delta N*} (X_4, X_5) \Psi_{\beta_k \beta_l \beta_m} (\tilde{X}_1, \tilde{X}_2, \tilde{X}_3).$$

Summing these formulas over the internal variables, we get the density matrix in the form of a sum of nine terms

$$\rho^\Delta (X_1, X_2, X_3; \tilde{X}_1, \tilde{X}_2, \tilde{X}_3) = \rho_{C\Delta N} + \rho_{C N\Delta} + \rho_{\Delta N C} + \rho_{N\Delta C} + \rho_{\Delta C C} + \rho_{N C C} + \rho_{C\Delta C} + \rho_{C N C} + \rho_{C C C}.$$

Here the subscripts define the state of the particles with the numbers 1, 2, and 3.

Recall that the exchange amplitude (1) is presented in the form in which the photon interacts with particle 1 while particles 2 and 3 go to a free state. Because of the orthogonality of the internal wave functions, the exchange amplitudes of the $A(\gamma, \pi NN)B$ process, corresponding to the matrices $\rho_{C\Delta N}$, $\rho_{C N\Delta}$, $\rho_{\Delta N C}$, $\rho_{C\Delta C}$, are zero. Amplitudes associated with the matrices $\rho_{\Delta C C}$, $\rho_{N C C}$, and $\rho_{C C C}$ answer to the reaction mechanism, in which the nucleons in a state lower than the Fermi level go to a free state. The probability of such processes with the nucleon momentum in excess of ~ 200 MeV/c is very small. Therefore, we ignore them. The remaining two matrices

$$\begin{aligned} \rho_{\Delta N C} (X_1, X_2, X_3; \tilde{X}_1, \tilde{X}_2, \tilde{X}_3) &= \frac{2}{A(A-1)(A-2)} \\ &\times \varphi_{\Delta N N} (m_1 m_2 m_3) \left[\sum_{ijk \neq ij} \Psi_{\beta_i \beta_j}^{\Delta N} (x_1 x_2) \Psi_{\beta_k} (x_3) \right. \\ &\quad \left. \times \Psi_{\beta_k}^* (\tilde{x}_3) \Psi_{\beta_i \beta_j}^{\Delta N*} (\tilde{x}_1 \tilde{x}_2) \right] \varphi_{\Delta N N}^* (\tilde{m}_1 \tilde{m}_2 \tilde{m}_3), \\ \rho_{C N C} (X_1, X_2, X_3; \tilde{X}_1, \tilde{X}_2, \tilde{X}_3) &= \frac{4}{A(A-1)(A-2)} \\ &\times \varphi_{N N N} (m_1 m_2 m_3) \left[\int d(x_4) \sum_{ij,kl \neq ij} \Psi_{\beta_i \beta_j}^{\Delta N} (x_4 x_2) \Psi_{\beta_k \beta_l} (x_1 x_3) \right. \\ &\quad \left. \times \Psi_{\beta_k \beta_l}^* (\tilde{x}_1 \tilde{x}_3) \Psi_{\beta_i \beta_j}^{\Delta N*} (x_4 \tilde{x}_2) \right] \varphi_{N N N}^* (\tilde{m}_1 \tilde{m}_2 \tilde{m}_3) \end{aligned}$$

correspond to the reaction mechanisms, which are illustrated by the diagrams in Fig. 2. Common to these two matrices is that the nucleon of the ΔN system goes to a free state.

5 Analysis of experimental data

At present, the experimental data of the $A(\gamma, \pi NN)B$ reaction are practically absent. Therefore, to compare the predictions of our model with experimental data, we will use the $A(\gamma, \pi N)$ reaction measured in the kinematic region where, according to [7], the pion production occurs in the $A(\gamma, \pi N)NB$ reaction with the emission of two nucleons. This kinematic region is characterized primarily by the large momentum transfers to the NB system, consisting of the free nucleon and the residual nucleus.

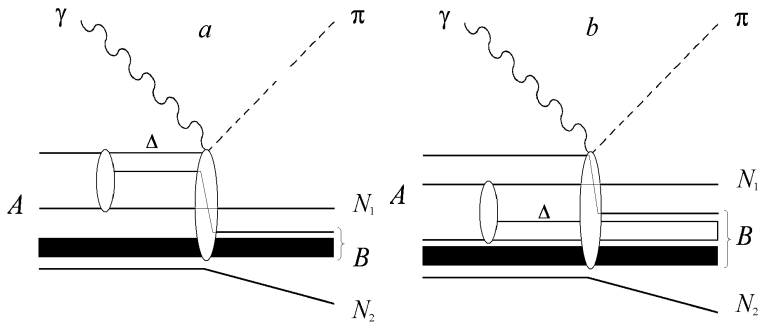


Figure 2: Diagrams illustrating the exchange mechanisms of the pion photoproduction on nuclei in the $A(\gamma, \pi NN)B$ reaction.

We will consider the data from two experiments carried out at the Tomsk synchrotron in which the $^{12}\text{C}(\gamma, \pi^-p)$ [7] and $^{12}\text{C}(\gamma, \pi^+p)$ [8] reactions were examined. Both experiments were performed in the kinematic region of the large momentum transfers to the residual system and have repeatedly attracted attention [2, 3, 9, 10]. The data of the $^{12}\text{C}(\gamma, \pi^-p)$ reactions are interesting in that at large opening angles of the pion-proton pair the maximum of the cross-section is observed, which has been interpreted as a manifestation of a quasi-bound isobar-nuclear state – a highly excited state of the nucleus which decays with the emission of the pion and nucleon [7, 9, 10]. The second $^{12}\text{C}(\gamma, \pi^+p)$ reaction, which is forbidden for the quasi-free pion photoproduction mechanism, is useful to study the isobar configuration in the ground state of the nucleus.

The experimental point in Fig. 3 is the differential cross-section, measured by using the bremsstrahlung beam of electrons in the two runs with electron beam energies of 500 and 420 MeV [8]. The measurements were performed by the simultaneous detection of a positive pion and a proton. Positive pions were detected at an angle of 54° to the photon beam axis. In Fig. 3 both the experimental data and the calculated cross-section are averaged over the proton energy in the interval of 80-120 MeV, over the pion energy in the interval of 71.5-106.5 MeV, and over the proton polar angle in the interval of $56-94^\circ$. In the kinematic region under consideration, the average photon energy and the average residual nucleus momentum were 355 MeV and 300 MeV/ c , respectively. Supposing that the pion production is in the $^{12}\text{C}(\gamma, \pi^+p)^{11}\text{Be}$ reaction, the cross-section was calculated on the basis of data on the differential yield of the reaction.

The theoretical differential cross-section of the $^{12}\text{C}(\gamma, \pi^+p)^{11}\text{Be}$ reaction depending on the energy of the proton is shown in Fig. 3 by a dashed-dotted curve. Using a model that takes into account the isobar configuration in the ground state of the nucleus, the calculations are performed. The wave function of the nucleon bound state is calculated using the harmonic-oscillator shell model which reproduces the charge radius of the ^{12}C nucleus. Final-state interaction is taken into account through an optical model. The model is described in detail in [2, 3]. As can be seen, the calculated cross-section of the $^{12}\text{C}(\gamma, \pi^+p)^{11}\text{Be}$ reaction is about ~ 0.1 of the experimental cross-section.

The dashed and dotted curves in Fig. 3 show the $d^3\tilde{\sigma}_{\pi N}$ contributions to the experimental cross-section of the $^{12}\text{C}(\gamma, \pi^+p)$ reaction of the events from the $^{12}\text{C}(\gamma, \pi^+p)NB$ reaction, in which the residual nuclear system NB contains a nucleon in a free state. The contribution

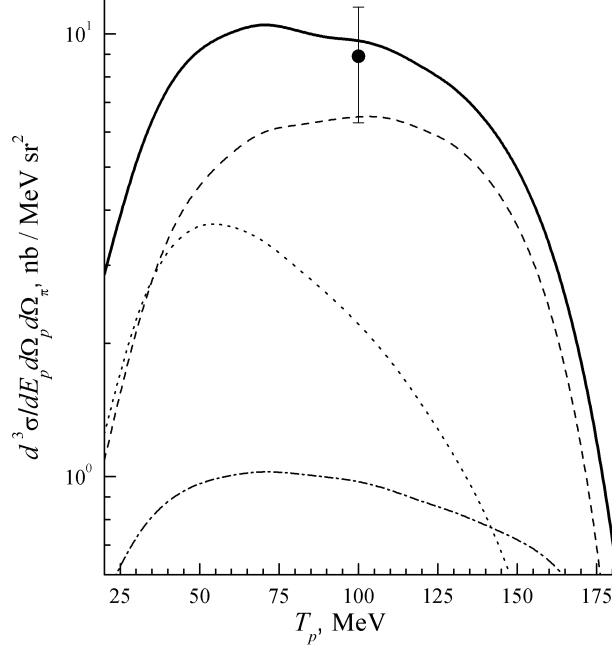


Figure 3: Differential cross-section of the $^{12}\text{C}(\gamma, \pi^+p)$ reaction for $\bar{E}_\gamma = 355$ MeV versus the kinetic energy of the proton T_p . Dashed-dotted curve: cross-section of the $^{12}\text{C}(\gamma, \pi^+p)^{11}\text{Be}$ reaction; dashed curve: summed contribution to the $^{12}\text{C}(\gamma, \pi^+p)NB$ reactions from the mechanisms, corresponding to the diagrams in Figs. 1a and 1b; dotted curve: summed contribution to the $^{12}\text{C}(\gamma, \pi^+p)NB$ reactions from the mechanisms, corresponding to the diagrams in Figs. 1d, 2a, and 2b; solid curve: total contribution to the cross-section of the $^{12}\text{C}(\gamma, \pi^+p)^{11}\text{Be}$, $^{12}\text{C}(\gamma, \pi^+p)n^{10}\text{Be}$, and $^{12}\text{C}(\gamma, \pi^+p)p^{10}\text{Li}$ reactions; data are taken from Ref. [8].

$d^3\tilde{\sigma}_{\pi N}$ is related with the cross-section $d^5\sigma_{\pi NN}$ of the $^{12}\text{C}(\gamma, \pi^+p)NB$ reaction by the relation

$$\frac{d^3\tilde{\sigma}_{\pi N}}{dE_p d\Omega_p d\Omega_\pi} \left| \frac{\partial E_\gamma}{\partial E_\pi} \right| f(E_\gamma) = \int dE'_\gamma d\Omega_N f(E'_\gamma) \frac{d^5\sigma_{\pi NN}}{dE_p d\Omega_p dE_\pi d\Omega_\pi d\Omega_N},$$

where $f(E_\gamma)$ is the bremsstrahlung spectrum of the electrons. The kinematic variables in the left side of this formula satisfy the law of energy and momentum conservation in the $^{12}\text{C}(\gamma, \pi^+p)^{11}\text{Be}$ reaction.

In the chosen kinematic region, the main factors determining the proton energy dependence of the cross-section of the $^{12}\text{C}(\gamma, \pi^+p)NB$ reaction are the momentum distributions of the isobar and the nucleon of the ΔN system in the nucleus. The influence that these factors have on the cross-section depends on the reaction mechanism. Dashed and dotted curves in Fig. 3 show the summed cross-section contributions from the reaction mechanisms, corresponding to the two groups of diagrams. The first group includes the diagrams in Figs. 1a and 1b, and the second, the diagram in Figs. 1d, 2a, and 2b. The main difference between these diagrams is that in the first group the proton of the πN -pair is the product of the $\gamma\Delta^{++} \rightarrow \pi^+p$ transition while in the second group the proton is the nucleon of the ΔN system. It should be noted that the amplitude of the reaction, corresponding to the diagram in Fig. 1a, includes both the $\gamma\Delta^{++} \rightarrow \pi^+p$ transition and the $\gamma\Delta^+ \rightarrow \pi^+n$ transition. However, the $\gamma\Delta^{++} \rightarrow \pi^+p$ transition is dominant. The position of the cross-section

maximum, represented by the dashed and dotted curves, is determined mainly by the dependence on the momentum of the Fourier transform of the wave function $\Psi^{\Delta N}$, describing the relative motion of the nucleon and the isobar of the ΔN system, which has a maximum at a momentum of 320 MeV/ c . The solid curve in Fig. 3 shows the total contribution to the cross-section of the $^{12}\text{C}(\gamma, \pi^+p)^{11}\text{Be}$, $^{12}\text{C}(\gamma, \pi^+p)n^{10}\text{Be}$, and $^{12}\text{C}(\gamma, \pi^+p)p^{10}\text{Li}$ reactions. In the kinematic region under consideration the mechanism corresponding to the diagram in Fig. 1*b* dominates. As can be seen, the calculated cross-section is in good agreement with the experimental data.

Figure 4 shows the differential yield of the $^{12}\text{C}(\gamma, \pi^-p)$ reaction depending on the opening angle $\Theta_{\pi p}$ of the pion and proton [7]. Experimental data were obtained under the following conditions. Pions with momentum 224 MeV/ c were detected at an angle of 76° with respect to the axis of the photon beam. The measurement results are averaged over the proton energy range 60-140 MeV. The experiment was performed at the bremsstrahlung beam of the electrons with an energy of 500 MeV.

The short dashed curve in Fig. 4, representing the yield of the reaction $^{12}\text{C}(\gamma, \pi^-p)^{11}\text{C}$ in the quasi-free approximation [11], satisfactorily describes the exponential decrease of the reaction yield with increases in the opening angle up to $\Theta_{\pi p} \simeq 150^\circ$. With further increases in $\Theta_{\pi p}$, a sharp disagreement takes place between the experimental and calculated data. The dashed-dotted curve in Fig. 4 shows the contribution of the isobar configuration in the ground state of ^{12}C to the yield of the $^{12}\text{C}(\gamma, \pi^-p)^{11}\text{C}$ reaction, which at a high opening angle is not more than 10^{-2} of the experimental cross-section [2]. The dashed, dotted, and dash-dot-dot curves represented in Fig. 4 are the sums of the contributions from the mechanisms of the $^{12}\text{C}(\gamma, \pi^-p)NB$ reaction, corresponding to the three groups of diagrams, which lead to the cross-sections with the different angular correlations.

The first group includes the diagrams in Figs. 1*b* and 1*c*. The contribution to the reaction yield of these diagrams is shown in Fig. 4 by the dashed curve. In this case, the angular correlation of the reaction yield is due to the strong dependence of the momentum of the pion-proton pairs and, therefore, the active baryon momentum in the initial state $\mathbf{p}_B = \mathbf{p}_\pi + \mathbf{p}_p - \mathbf{p}_\gamma$ from the opening angle $\Theta_{\pi p}$ of the pion and proton. The maximum of the angular dependence of the reaction yield, associated with the first group of diagrams, has the same nature as the maximum of the cross-section of the $^{12}\text{C}(\gamma, \pi^+p)NB$ reaction, shown in Fig. 3 by the dashed curve. At the opening angle $\Theta_{\pi p} \simeq 150^\circ$ the mean momentum is $|p_B| \simeq 320$ MeV/ c . The second group includes the diagrams in Figs. 1*a*, 2*a*, and 2*b*. The diagram in Fig. 1*a* contains $\gamma\Delta^0 \rightarrow \pi^-p$ and $\gamma\Delta^- \rightarrow \pi^-n$ transitions. The last transition, at which the proton is a nucleon of the ΔN system, dominates. Therefore, we have included this diagram in the second group. In the amplitudes corresponding to the diagrams of the second group, the escape directions of the pion and proton are dynamically weakly correlated. The reaction yield contribution of this group's diagrams is shown in Fig. 4 by the dotted curve. The observed slight decrease in yield of the reaction with increasing opening angle mainly has the phase-space nature.

The third group includes the diagram in Fig. 1*d*. The contribution of this diagram to the yield of the $^{12}\text{C}(\gamma, \pi^-p)n^{10}\text{C}$ reaction is concentrated in the region of low momentum of the residual nuclear system $n^{10}\text{C}$, where the quasi-free mechanism of the $^{12}\text{C}(\gamma, \pi^-p)^{11}\text{C}$ reaction dominates. In the case of the $^{12}\text{C}(\gamma, \pi^-p)p^{10}\text{B}$ reaction, the amplitude, corresponding to the diagram in Fig. 1*d*, includes an additional component, in which the proton of the π^-p pair is a nucleon of the ΔN system. This component of the amplitude in properties is similar to the amplitudes of the second diagram group, which have weak angular

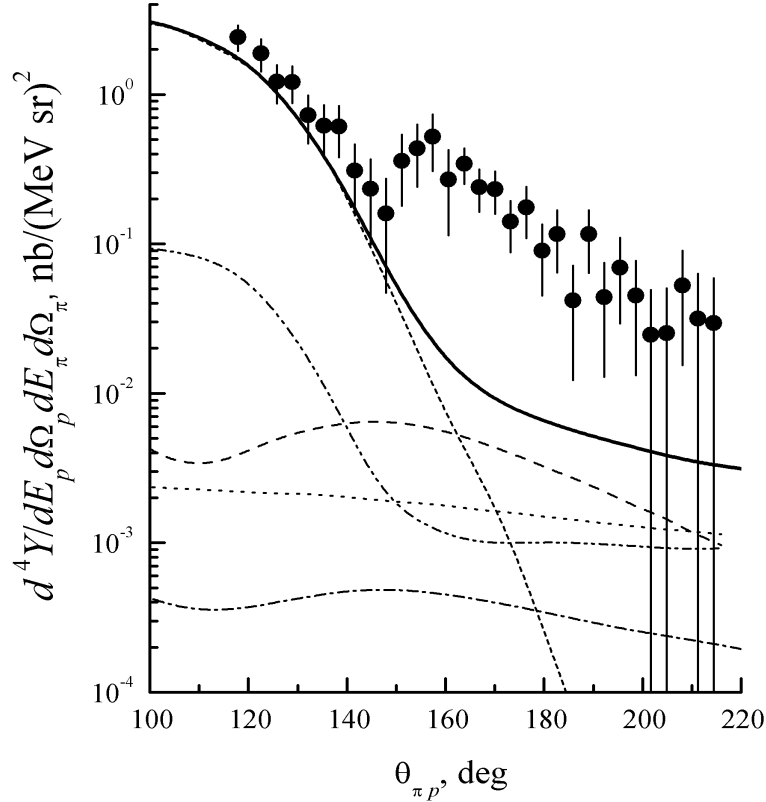


Figure 4: Differential yield of the $^{12}\text{C}(\gamma, \pi^-p)$ reaction versus the $\Theta_{\pi p}$ opening angle. Short dashed curve: quasi-free pion photoproduction in the $^{12}\text{C}(\gamma, \pi^-p)^{11}\text{C}$ reaction; dashed-dotted curve: the contribution of the isobar configuration in the ^{12}C ground state to the yield of the $^{12}\text{C}(\gamma, \pi^-p)^{11}\text{C}$ reaction; dashed curve: summed contribution from the mechanisms of the $^{12}\text{C}(\gamma, \pi^-p)NB$ reactions, corresponding to the diagrams in Figs. 1b and 1c; dotted curve: summed contribution from the mechanisms of the $^{12}\text{C}(\gamma, \pi^-p)NB$ reactions, corresponding to the diagrams in Figs. 1a, 2a, and 2b; dashed-dotted-dotted curve: the contribution from the mechanism of the $^{12}\text{C}(\gamma, \pi^-p)NB$ reactions, corresponding to the diagram in Fig. 1d; solid curve: total contribution of the $^{12}\text{C}(\gamma, \pi^-p)^{11}\text{C}$, $^{12}\text{C}(\gamma, \pi^-p)n^{10}\text{C}$, and $^{12}\text{C}(\gamma, \pi^-p)p^{10}\text{B}$ reactions; data are taken from Ref. [7].

dependence. The contribution to the yield of the reaction diagram in Fig. 1d is shown in Fig. 4 by the dash-dot-dot curve.

The total contribution to the reaction yield of the π^-p pair produced in the $^{12}\text{C}(\gamma, \pi^-p)^{11}\text{C}$, $^{12}\text{C}(\gamma, \pi^-p)n^{10}\text{C}$, and $^{12}\text{C}(\gamma, \pi^-p)p^{10}\text{B}$ reactions is shown in Fig. 4 by the solid curve. For the $^{12}\text{C}(\gamma, \pi^-p)n^{10}\text{C}$ reaction the mechanism, corresponding to the diagram in Fig. 1c, dominates at the opening angle $\Theta_{\pi p} \simeq 180^\circ$. As can be seen, for the large scattering angles calculated, the reaction yield is an order of magnitude less than that of the experimental data.

6 Conclusion

We have presented a model of the pion photoproduction on the nucleus with the emission of two nucleons in the $A(\gamma, \pi NN)B$ reaction. In this model we have moved beyond the

standard shell-model considering ΔN correlations in the nuclear wave functions, which are caused by the virtual transitions $NN \rightarrow \Delta N \rightarrow NN$ in the ground state of the nucleus. The main ingredients of the model are the two- and three-particle density matrixes and the transition operators $\gamma\Delta \rightarrow N\pi$ and $\gamma N \rightarrow N\pi$. The direct and exchange reaction mechanisms, which follow from the structure of the density matrixes, were examined. This model is an extension of our recent model for the $A(\gamma, \pi N)B$ reaction [2] to the pion photoproduction in the $A(\gamma, \pi NN)B$ reaction.

The processes of pion production in the $^{12}\text{C}(\gamma, \pi^+p)$ and $^{12}\text{C}(\gamma, \pi^-p)$ reactions were considered. The analysis of these reactions is made in the kinematic region of the large momentum transfers to the residual nuclear system. The motivation for this work is based on the conclusion drawn in [2] that it is impossible to explain experimental data of the $^{12}\text{C}(\gamma, \pi^+p)$ [8] and $^{12}\text{C}(\gamma, \pi^-p)$ [7] reactions assuming that the residual nuclei are in a bound state in these reactions.

The experimental data of the $^{12}\text{C}(\gamma, \pi^+p)$ reaction [8] were explained satisfactorily by the total contribution of the $^{12}\text{C}(\gamma, \pi^+p)^{11}\text{Be}$, $^{12}\text{C}(\gamma, \pi^+p)n^{10}\text{Be}$, and $^{12}\text{C}(\gamma, \pi^+p)p^{10}\text{Li}$ reactions, using the reaction mechanisms due to ΔN -correlations. It is shown that at the large momentum transfer the photoproduction of the pions on the nucleus with the emission of two nucleons is dominant. It was found that the (γ, π^+p) reaction is not very sensitive to the parameters of the wave function of the ΔN system in the studied kinematic region, but it allows us to estimate the probability of the virtual $NN \rightarrow \Delta N$ transition. In our model, the probability of the isobar configurations in the ^{12}C ground state per nucleon is 0.0126, which is consistent with the experimental data of [8].

The results of an estimation of the isobar configuration contribution in the cross-section of the $^{12}\text{C}(\gamma, \pi^-p)$ reaction are interesting in another aspect. The considered mechanisms of the pion-nucleon pair production can be background or imitative in relation to the processes that are accompanied by the excitation of the hypothetical highly excited nucleus states [10]. According to our analysis, the cross-section of the $^{12}\text{C}(\gamma, \pi^-p)$ reaction, measured in the experiment [7] at large opening angles of the pion and proton, cannot be explained by the contribution of the isobar configurations in the ^{12}C ground state. So, the question, brought up at different times in [7, 9, 10, 12, 13], about the existence of the resonance and bound isobar-nuclear states that decay with the emission of the pion-nucleon pair remains open.

References

- [1] R. Shneor, P. Monaghan, R. Subedi, et al., Phys. Rev. Lett. 99 (2007) 072501.
- [2] I.V. Glavanakov, A.N. Tabachenko, Nucl. Phys. A 889 (2012) 51.
- [3] I.V. Glavanakov, A.N. Tabachenko, Phys. At. Nucl. 75 (2012) 1019.
- [4] G. Horlacher, H. Arenhovel, Nucl. Phys. A 300 (1978) 348.
- [5] A.N. Tabachenko, Russ. Phys. J. 50 (2007) 303.
- [6] I. Blomqvist, J.M. Laget, Nucl. Phys. A 280 (1977) 405.
- [7] I.V. Glavanakov, Yu.F. Krechetov, O.K. Saigushkin, et al., JETP Lett. 81 (2005) 432.
- [8] V.M. Bystritsky, A.I. Fix, I.V. Glavanakov, et al., Nucl. Phys. A 705 (2002) 55.

- [9] I.V. Glavanakov, Yu.F. Krechetov, *Phys. At. Nucl.* 71 (2008) 413.
- [10] I.V. Glavanakov, *Phys. At. Nucl.* 72 (2009) 1823.
- [11] I.V. Glavanakov, *Sov. J. Nucl. Phys.* 49 (1989) 58.
- [12] P. E. Argan, G. Audit, N. De Botton, et al., *Phys. Rev. Lett.* 29 (1972) 1191.
- [13] P. Bartsch, D. Baumann, J. Bermuth, et al., *Eur. Phys. J. A* 4 (1999) 209.